Human Pathology (2020) **104**, 30–41

ELSEVIER

Human PATHOLOGY

www.elsevier.com/locate/humpath

Original contribution

New molecular insights into the pathogenesis of lipoblastomas: clinicopathologic, immunohistochemical, and molecular analysis in pediatric cases☆,☆☆,☆☆☆

Oscar Lopez-Nunez MD [a,d], Rita Alaggio MD [b,c], Sarangarajan Ranganathan MD [b,d], Lori Schmitt HTL [e], Ivy John MD [a,b], Alanna J. Church MD [f,1], Jennifer Picarsic MD [b,d,*,1]

[a] *Department of Pathology and Laboratory Medicine, UPMC, Pittsburgh, PA, 15213, USA*
[b] *Department of Pathology, University of Pittsburgh School of Medicine, Pittsburgh, PA, 15213, USA*
[c] *Department of Pathology, Bambino Gesù Children's Hospital, IRCCS, Rome, 00165, Italy*
[d] *Division of Pathology and Laboratory Medicine, Cincinnati Children's Hospital Medical Center, Cincinnati, OH, 45229, USA*
[e] *Division of Pediatric Pathology, UPMC Children's Hospital of Pittsburgh, Pittsburgh, PA, 15224, USA*
[f] *Department of Pathology, Boston Children's Hospital, Boston, MA, 02115, USA*

Received 29 May 2020; revised 14 July 2020; accepted 14 July 2020

Available online 18 July 2020

Keywords:
Lipoblastoma;
Lipoma;
Myxoid liposarcoma;
PLAG1;
HMGA2;
FISH;
RNA sequencing

Summary Lipoblastomas can occasionally require further molecular confirmation when occurring outside of the usual age groups or demonstrating unusual morphology. We reviewed 28 lipoblastomas with 16 controls. Lipoblastomas were subdivided into myxoid (n = 7), classic (n = 9), or lipoma-like (n = 12) subtypes. PLAG1 immunohistochemistry, *PLAG1* fluorescence in situ hybridization (FISH), and targeted RNA sequencing were performed on formalin-fixed paraffin-embedded tissue. Karyotypes were available in a subset of lipoblastomas (n = 9). Gene rearrangements were identified in 17/25 (68%) lipoblastomas, including *PLAG1* (15/25, 60%) and *HMGA2* (2/25, 8%). Five novel fusion partners (*DDX6*, *KLF10*, and *KANSL1L* with *PLAG1* and *EP400* and *FGD6* with *HMGA2*) were found. PLAG1 immunohistochemistry was positive (nuclear, moderate/strong) in myxoid and classic subtypes lipoblastomas with preferential expression in mesenchymal cells within myxoid stroma and fibrous

☆ An abstract of this work was presented at the 2017 Society for Pediatric Pathology Fall meeting in Denver, Colorado.

☆☆ Competing interests: None

☆☆☆ Funding/Support: This work was supported by the National Institutes of Health Grants UL1TR000005 and CA88041 and also by the Department of Pathology, University of Pittsburgh School of Medicine and University of Pittsburgh Medical Center , where Dr. Jennifer Picarsic is currently now an Adjunct Associate Professor.

* Corresponding author. Cincinnati Children's Hospital Medical Center, Department of Pathology and Laboratory Medicine, 3333 Burnet Ave., ML 1035, Cincinnati, OH, 45229, USA.
E-mail address: jenpicarsic@gmail.com (J. Picarsic).

[1] Both authors share equal contribution as senior authors.

https://doi.org/10.1016/j.humpath.2020.07.016

septa and negative in all controls. When comparing PLAG1 immunohistochemistry with molecular testing (FISH and/or RNA sequencing and/or karyotype), concordant results were noted in 13/25 (52%) cases, increasing to 15/25 (60%) after slight adjustment of the *PLAG1* FISH positive threshold. In myxoid and classic lipoblastomas, PLAG1 immunohistochemistry seems to be a better surrogate marker for *PLAG1* rearrangement, as compared with lipoma-like subtypes. In lipoma-like subtypes, targeted RNA sequencing appears to detect *PLAG1* fusions better than FISH and immunohistochemistry. The preferential expression of PLAG1 in the mesenchymal and fibroblast-like cells deserves further investigation as the putative cell of origin in lipoblastoma.

1. Introduction

Lipoblastomas are benign neoplasms composed of primitive spindled mesenchymal cells, lipoblasts, and mature adipocytes with variable myxoid stroma and delicate vasculature [1]. These tumors exhibit a slight male predominance and usually present under the age of 5 years [2,3]. However, they can also affect young adults in the second decade of life (10% of cases) with the potential for late recurrences [4].

Lipoblastomas can occasionally show unconventional morphology or affect unusual age groups requiring confirmation of the *PLAG1* fusion gene [2−9]. This can be accomplished via fluorescence in situ hybridization (FISH) by using *PLAG1* break-apart probes, which can be expanded by targeting other translocation-related neoplasms or by RNA sequencing studies [10]. In addition, PLAG1 immunohistochemistry represents a more cost-effective, first-line approach [9,11]; however, only a few studies have directly compared it to other molecular and cytogenetic techniques, most of which are limited to case reports [2,12−14].

Interestingly, alternative mechanisms such as polysomy 8 have been seen in a subset of lipoblastomas (9−18%), either alone or in combination with *PLAG1* fusions [6]. Likewise, *PLAG1* rearrangements were reported in 2% of lipomatous tumors from older patients (>15 years) lacking the conventional features of lipoblastomas, suggesting that *PLAG1*-rearranged lipomatous tumors may represent a distinct and broader pathologic entity, regardless of their phenotype [7]. Furthermore, a rare *HMGA2*-rearranged lipoblastoma has also been reported [15]. Clearly, our understanding of the underlying biologic mechanisms of lipomatous tumors is still limited and has not yet been studied in a large pediatric series. We aim to explore and offer new insights into the clinicopathological and biological features of lipoblastomas by using an integrative approach including morphologic, immunohistochemical, and molecular studies.

2. Materials and methods

2.1. Case selection

Twenty-eight pediatric lipoblastomas were retrieved from our archival material (2003−2018) after institutional review board approval. All cases were reviewed by 4 pediatric pathologists (O.L.N., R.A., S.R., and J.P.), and the lipoblastomas were subdivided into myxoid, classic, or lipoma-like morphology as previously described [6]. Additionally, 3 pediatric myxoid liposarcomas, 7 pediatric lipomas, and 6 primitive myxoid mesenchymal tumors of infancy (PMMTI) were selected as controls.

2.2. FISH and karyotype analysis

The interphase FISH analysis was conducted on formalin-fixed paraffin-embedded (FFPE) tissue sections. *PLAG1* rearrangement was detected by a dual-color break-apart probe (Empire Genomics, Buffalo, NY). Based on internal validation with salivary gland tumors, *PLAG1* FISH was considered positive if *PLAG1* break-apart signal was present in ≥9.93% of cells in a minimum of 60 analyzed cells (positive control: salivary gland tumor), similar to the positive threshold set by salivary gland tumors (19) and internal validations. The monolayer cell cultures were harvested from surgical specimens, and karyotypes were described by institutional standard protocols.

2.3. Targeted RNA sequencing

Total nucleic acid (DNA and RNA) extracted from FFPE tissue using the Promega Maxwell RSC instrument and reagents (Madison, WI). Nucleic acid quantitation was performed with the Promega Quantus fluorometer using the RNA QuantiFluor kit (Madison, WI). Library preparation uses the anchored multiplex PCR technique (ArcherDX, Boulder, CO), as previously described [16], which allows for the alignment and detection of any fusion partner connected to a target gene. RNA quality/integrity was

Table 1 Clinicopathologic features of 28 lipoblastomas.

Case	Age (years)	Sex	Location	Size (cm)
Myxoid lipoblastoma (n = 7), median age: 1-year, median size: 7.0 cm				
2	3	F	Upper extremity	N/A[a]
3	1	M	Head and neck	9.7
6	0.7	M	Lower extremity	4
7	1	F	Lower extremity	10.4
8	0.1	F	Trunk	7
15	0.1	F	N/A	7
16	1	M	Retroperitoneum	5.5
Classic lipoblastoma (n = 9), median age: 3 years, median size: 5.5 cm				
1	2	M	Trunk	5.5
4	2	F	Lower extremity	8
5	1	F	Lower extremity	2
9	9	M	Trunk	5.6
10	4	F	Lower extremity	3.8
11	14	M	Lower extremity	2
12	7	M	Trunk	9
13	3	F	Head and neck	5
14	3	F	Trunk	11.5
Lipoma-like lipoblastoma (n = 12), Median age: 5.5 years, median size 6.5 cm				
17	13	F	Lower extremity	2.8
18	13	M	Trunk	8.7
20	0.5	M	Trunk	7
22	1	F	Upper extremity	5.3
23	5	F	Upper extremity	5
24	3	M	Lower extremity	3
25	2	M	Trunk	7.7
26	8	F	Upper extremity	5.8
27	10	M	Trunk	12.2
28	9	F	Trunk	6.1
29	6	M	Trunk	10
34	5	F	Trunk	15

Abbreviations: N/A, not available; F, Female; M, Male.
[a] Recurrence.

assessed before library preparation by a quantitative PCR (qPCR)-based, PreSeq QC Assay using the iTaq SYBR Green Supermix from Bio-Rad (Hercules, CA) and 10x VCP primers from ArcherDX. Final library quantification was achieved by using a qPCR-based, KAPA Library Quantification Kit for Illumina® Platforms from KAPA Biosystems (Wilmington, MA). Each case underwent targeted RNA sequencing on a custom-designed panel of 64 genes, including *PLAG1* and *HMGA2*. Sequencing was performed in an Illumina MiSeq instrument (San Diego, CA). Data analysis was conducted using the ArcherAnalysis bioinformatics software system (ArcherDX) and was interpreted by a molecular pathologist (A.C). The genetics analyses were performed on the Solid and Brain Tumor assay at the Laboratory for Molecular Pediatric Pathology at Boston Children's Hospital, which was subsequently validated according to the standards and guidelines of the Association for Molecular Pathology [17,18] and in keeping with the CLIA regulations, as previously described [19].

2.4. Immunohistochemistry

Immunohistochemistry was performed on 3 μm thick FFPE sections using commercially available antibodies for PLAG1 (clone 3B7, Novusbio, Littleton, CO), desmin (clone DE-R-11, Ventana Medical Systems, Tucson, AZ), CD34 (QBEnd-10 clone from DAKO with mild antigen retrieval), and HMGA2 (GTX100519, polyclonal, GeneTex, Irvine, CA). PLAG1, CD34, and desmin slides were stained using the Ventana Ultra automated staining platform and respective proprietary reagents and DAB detection kits, and HMGA2 slides were done on Leica Bond with proprietary reagents. A molecularly confirmed lipoblastoma was used as a positive control. The PLAG1 immunohistochemistry was graded per the percentage of positive nuclei as follows: 0 (no staining), 1+(<10% cells), and 2+(≥10% cells) as well as the intensity of staining (negative, weak, moderate or strong) similar to the grading system described by Rotellini et al in salivary gland tumors [11]. We considered any staining (ie ≥1+) with moderate to strong intensity, as positive PLAG1 expression. The HMGA2 (nuclear), CD34 (cytoplasmic), and desmin (cytoplasmic) immunohistochemistry were also scored similarly. Staining expression was recorded in adipocytes and mesenchymal cells in the fibrous septa or myxoid stroma.

3. Results

3.1. Clinical and morphological features

The clinicopathological features of the lipoblastoma group (n = 28) are detailed in Table 1. The tumors occurred in 13 males and 15 females (M:F ratio 0.9), ranging in age from 1 month to 22 years (median 3 years, mean 4.5 years). No syndromic associations were found in any of our patients with lipoblastomas. Additional details are provided in Table 1 and Supplemental Table 2 for controls.

Macroscopically, myxoid lipoblastomas revealed a yellow to white tissue admixed with variably gelatinous areas (Fig. 1A, Case 2). Classic (Fig. 1B) and lipoma-like (Fig. 1C) lipoblastomas showed a more homogeneous gross appearance composed of yellow tissue with variable intervening septa and focal areas of hemorrhage. Histologically, all lipoblastomas were lobulated with intervening fibrous septa, regardless of histologic subtype. All myxoid lipoblastomas (n = 7) were variably cellular with a myxoid background comprising >50% of the specimen including focal pools of mucin, primitive stellate to spindled mesenchymal cells, minimal adipocytic elements, and absent mitotic activity (Fig. 1D) with plexiform vasculature

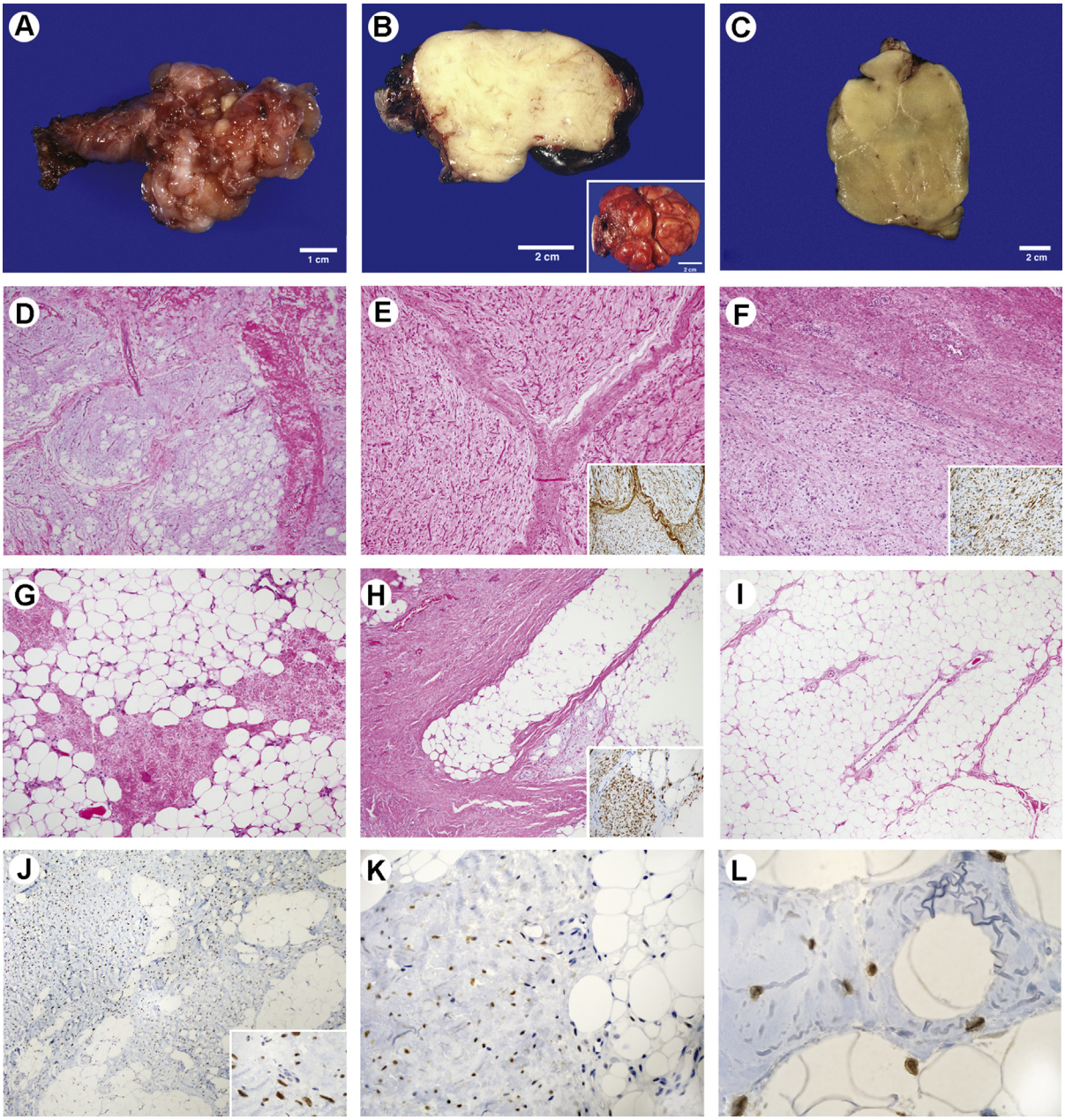

Fig. 1 Pathology of lipoblastomas. Gross images of myxoid (A), classic (B), and lipoma-like (C) lipoblastomas. Histopathology of myxoid lipoblastomas (D, H&E 10x; E, H&E 10x; F, H&E 20x) with unusual variants: E: Case 15 with prominent mesenchymal spindle cells and mild atypia with one lacking apparent lipoblasts and strong CD34 expression in the spindled cells (inlet, CD34 immunohistochemistry 10x) and negative desmin (not shown) and F: Case 2, a recurrence, with scant lipoblasts and hypercellular spindled mesenchymal areas in a prominent collagenized stroma with strong desmin expression in spindled mesenchymal cells (inlet, desmin immunohistochemistry 10x) and negative CD34 (not shown). Histopathology of classic lipoblastomas (G, H&E 20x and H, H&E10x) with strong desmin expression in case 13 (inlet, desmin immunohistochemistry 10x). Histopathology of lipoma-like lipoblastomas (I, H&E, 10x). The expression of PLAG1 immunohistochemistry in lipoblastomas (J, PLAG immunohistochemistry 10x, with inlet 100x) (K, PLAG immunohistochemistry 40x) (L, PLAG immunohistochemistry 100x) lipoblastomas.

reminiscent of myxoid liposarcomas. Two myxoid lipoblastomas had prominent mesenchymal spindle cells with mild atypia; one lacking apparent lipoblasts (Fig. 1E, Case 15), whereas the other was a recurrence with scant lipoblasts and hypercellular spindled mesenchymal areas in a prominent collagenized stroma (Fig. 1F, Case 2). Classic lipoblastomas (n = 9) had lobular architecture and variable amounts of mature adipose tissue with scattered lipoblasts, spindle cells, and myxoid stroma comprising <50% of the specimen (Fig. 1G–H). This subtype showed a variable

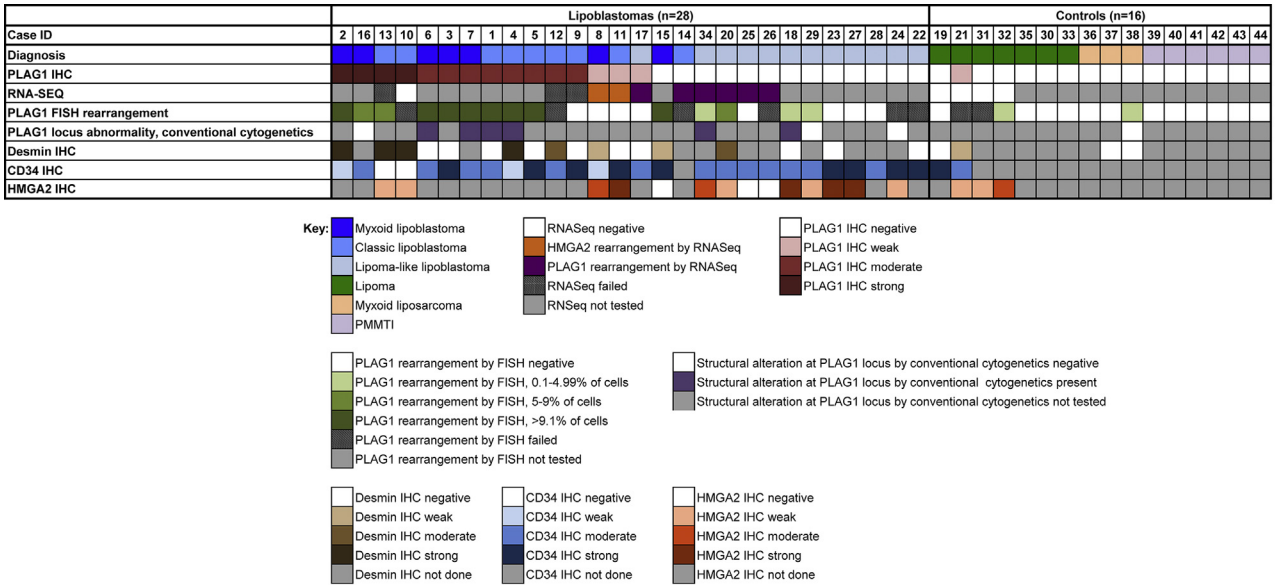

Fig. 2 Oncoprint-like map of lipoblastomas and controls with respect to diagnosis, immunohistochemistry, and molecular results. The key is color-coded. (For interpretation of the references to color in this figure legend, the reader is referred to the Web version of this article.) PMMTI, primitive myxoid mesenchymal tumor of infancy; IHC, immunohistochemistry; FISH, fluorescence in situ hybridization.

zonal pattern of "maturation" and less evident plexiform vasculature, mostly confined to myxoid areas. Two cases presented with mild focal cytologic atypia of primitive mesenchymal cells, resembling the so-called "ancient" change; however, no mitoses were identified. Lipoma-like lipoblastomas (n = 12) were largely composed of mature adipocytes of varying sizes surrounded by intervening fibrous septa and minimal to absent lipoblasts or myxoid stroma (Fig. 1I). Zonal "maturation" was observed in three lipoma-like lipoblastomas, and plexiform vasculature was focal in one case while absent in the remaining. No spindle cell component, atypia, or mitoses were identified in this subgroup.

3.2. Molecular features

3.2.1. Interphase FISH results

PLAG1 rearrangement was identified in 8 of 21 lipoblastomas (38%) using established criteria. Seven other cases were FISH failures. Additional details are provided in Fig. 2 and Supplemental Table 1 with representative FISH images in Fig. 3.

3.2.2. Targeted RNA sequencing

RNA sequencing revealed a *PLAG1* rearrangement in 6 of 9 (67%) lipoblastomas. RNA sequencing failed in the remaining 3 cases. Fusion partners included known (*HAS2*, *COL1A2*) and three novel partners (*DDX6*, *KLF10,* and *KANSL1L)*. Two of the 9 (22%) lipoblastomas harbored novel *HMGA2* fusions (partners *EP400* and *FGD6)*. No fusion genes were detected in the remaining case. Remarkably, 1 tumor (case 34) showed features of a conventional lipoma but was re-classified as lipoma-like

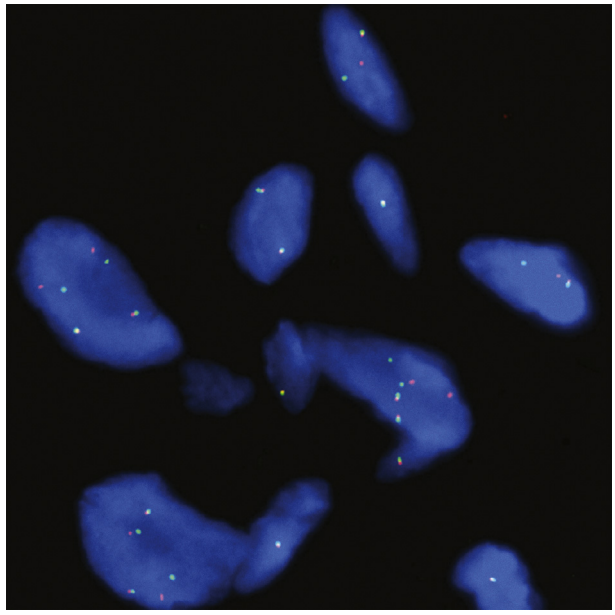

Fig. 3 *PLAG1* rearrangement was detected by a dual-color break-apart probe (Empire Genomics, Buffalo, NY). The *PLAG1* FISH was performed using 5-Fluorescein labeled RP11-22E14 and 5-TAMRA labeled RP11-1130K23, which hybridizes on either side of 8q12.1. (For interpretation of the references to color in this figure legend, the reader is referred to the Web version of this article.) FISH, fluorescence in situ hybridization.

lipoblastoma based on conventional karyotype findings and the presence of a *HAS2-PLAG1* rearrangement. RNA sequencing results are summarized in Fig. 2 and Supplemental Table 1 with the schematic of fusion partners in Fig. 4.

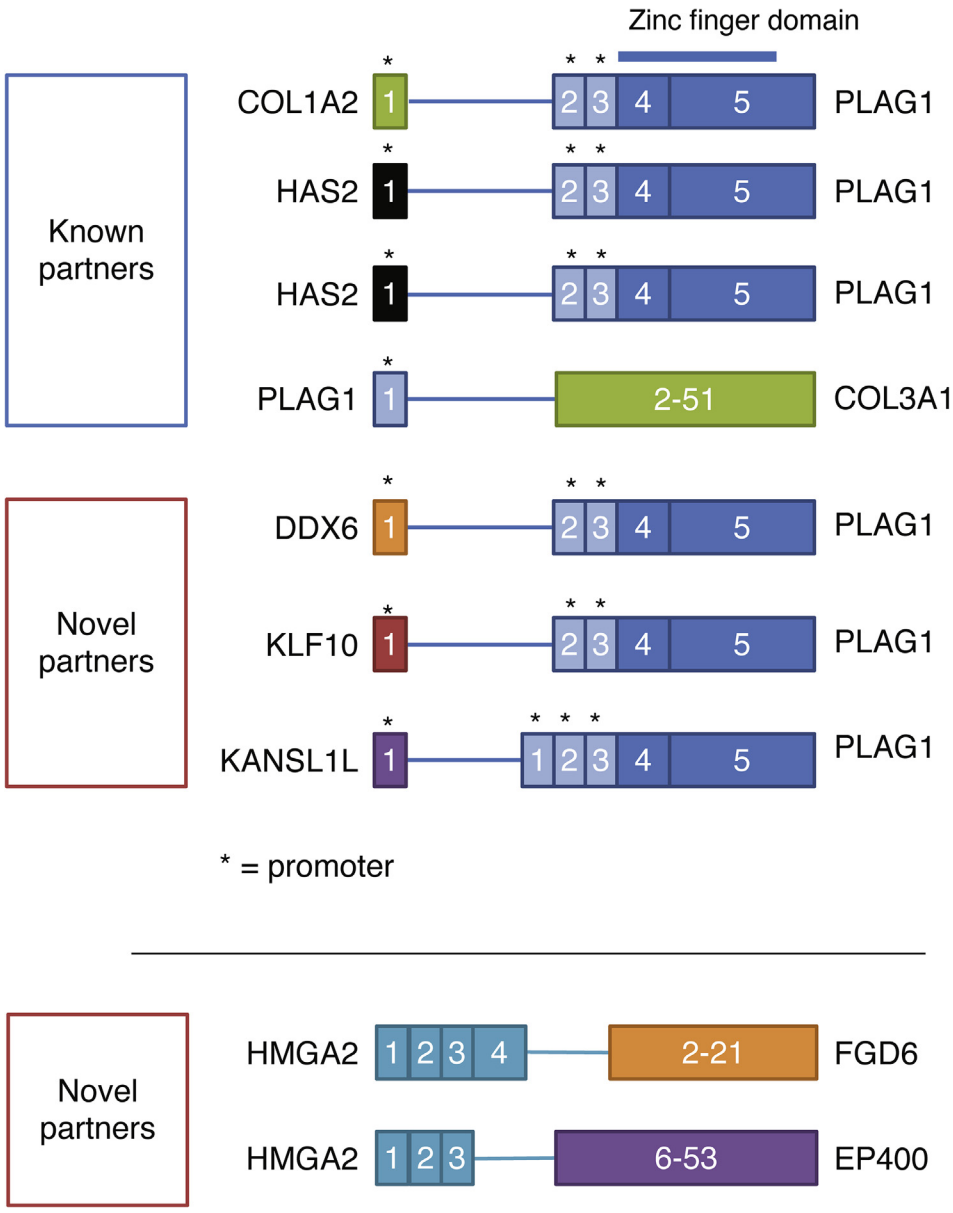

Fig. 4 Schematics of *PLAG1* fusions for lipoblastomas in this series using targeted RNA sequencing with anchored multiplex PCR technique (ArcherDX, Boulder, CO). Three novel *PLAG1* partners: *DDX6, KLF10, KANSL1L*; and 2 novel *HMGA2* partners: *EP400* and *FGD6* were identified.

3.2.3. Conventional cytogenetic karyotyping

Karyotype was available in 9 lipoblastomas. Six (67%) cases demonstrated structural alterations of 8q11-q13, of which 5 were also confirmed by either FISH or RNA sequencing. Three cases had no structural alterations of chromosome 8. Karyotype results are summarized in Fig. 2 and Supplemental Table 1.

3.3. Immunohistochemical features

3.3.1. PLAG1 immunohistochemistry

The PLAG1 immunohistochemistry results are summarized in Fig. 2 and Supplemental Table 1 with representative images in Fig. 1J-L. Briefly, PLAG1 nuclear staining was predominantly noted in primitive cells within the

myxoid stroma, including lipoblasts and spindle cells of fibrous septa, with none to minimal staining in adipocyte nuclei for most cases. PLAG1 immunostain was performed on all cases and was scored as moderate to strongly positive in 12 lipoblastomas (43%), including most myxoid (5/7) and classic (7/9) subtypes. Only one lipoma-like lipoblastoma showed focal weak expression that was interpreted as negative (Case 17). Two cases with focal weak PLAG1 expression harbored *HMGA2* rearrangements. All controls were negative.

3.3.2. HMGA2, desmin, and CD34 immunohistochemistry

Additional immunohistochemical results are outlined in Fig. 2. Briefly, HMGA2 was expressed in the 2 lipoblastomas harboring *HMGA2* translocations with moderate to strong nuclear reactivity in adipocytes and focal mesenchymal cells within the fibrous septa and myxoid stroma. Desmin was strongly and preferentially positive in mesenchymal cells within dense fibrous septa, in a subset of lipoblastomas showing PLAG1 expression, although no clear correlation was noted. The CD34 was positive in mesenchymal cells and blood vessels highlighting the zonal pattern, also without obvious correlation with PLAG1 expression.

Intriguingly, a group of lipoblastomas showed an inverse relation between desmin and CD34 immunophenotype with some cases displaying strong desmin and negative to weak CD34 (Cases 2, 4, 10, and 13) and a second subset exhibiting the opposite with strong CD34 and negative to weak desmin (Cases 3, 5, 9, 11, and 15). However, no direct correlation with myxoid or classic morphologic subtype was noted. PLAG1 immunohistochemistry was strongly positive in the first group with strong desmin, whereas variable in the second one. Among these cases, 2 *PLAG1*-rearranged myxoid lipoblastomas are particularly worthy of mention. The most primitive-appearing tumor with no apparent lipoblasts (Case 15, Fig. 1E) demonstrated diffuse CD34 expression in plump mesenchymal cells within a myxoid matrix (Fig. 1E, inset) and only focal weak desmin immunoreactivity. By contrast, a recurrent myxoid lipoblastoma (Case 2, Fig. 1F) demonstrated diffuse desmin expression in mesenchymal cells within the fibrous stroma (Fig. 1F, inset) but only focal weak CD34 expression limited to rare mesenchymal cells with "ancient-like" changes.

3.4. Morphologic, immunophenotypic, and molecular comparison

Diagnostic PLAG1 immunohistochemical and molecular results were available for direct comparison in 25 of the 28 (89%) lipoblastomas (Fig. 2 and Supplemental Table 1). Among those, there was concordant PLAG1 molecular and PLAG1 immunohistochemistry in 13 (52%) cases: 7 with concordant positive *PLAG1* rearrangement (confirmed by either FISH and/or targeted RNA sequencing and/or

Table 2 Differential diagnosis of lipoblastoma and key diagnostic features[a].

Lipoblastoma with a predominant myxoid morphology	
Myxoid liposarcoma	Rare in children, usually 3rd to 6th decades Peripheral concentration of mature adipocytes in lobules, focal nuclear atypia, pleomorphism, and abnormal mitoses Chromosome 12q13 (*CHOP*) rearrangement with translocation partners 16p11 (*FUS-TLS*) or 22p11 (*EWSR1*)
PMMTI	Infants Predominant round cell component, curvilinear-plexiform vascular pattern, pseudolipoblasts, cytologic atypia, frequent mitoses *BCOR*-ITD or *YWHAE* gene rearrangements
Lipoatrophy	Young and adults, clinical history of insulin-dependent diabetes mellitus or starvation (malnutrition or anorexia) Preserved lobular architecture, myxoid changes, pseudolipoblasts
Lipoblastoma-like tumor of vulva	Young and adult women Lobulated appearance, mature adipocytes interspersed with spindle cells, lipoblasts, myxoid stroma, branching vascular pattern, no zonal maturation pattern. Loss of RB protein expression or "mosaic pattern" by IHC No evidence of *PLAG1* genetic alterations
Lipoblastoma with a predominant mature lipomatous morphology	
Lipofibromatosis	Infants (subset congenital) up to early second decade Infiltrative pattern with entrapment of skeletal muscle, spindle cell component forming thin fascicles, mature adipose tissue, no lipoblasts Molecularly heterogeneous entity: activation of the *PI3K/AKT/mTOR* pathway (*EGF, HBEGF, TGF-α*), *EGFR* (*HER1*) or *EGFR*, or *ROS1*, *RET*, *PDGFRB*, may suggests pathogenesis of lipofibromatosis
Fibrous hamartoma of infancy	Infants Organoid growth pattern, spindle cell fascicles, primitive mesenchymal cells and mature adipose tissue, no lipoblasts/pseudolipoblasts EGFR positive expression by IHC *EGFR* exon 20 insertion/duplication mutations

Abbreviations: PMMTI, primitive myxoid mesenchymal tumor of infancy; IHC, immunohistochemistry.

PI3K/AKT/mTOR = Phosphatidylinositol 3-kinase-AKT-mammalian target of rapamycin; EGF = Epidermal Growth Factor; HBEGF = Heparin Binding EGF Like Growth Factor; TGF-a = Transforming growth factor alpha; EGFR (HER1) = Epidermal Growth Factor Receptor (Human epidermal growth factor receptor 1); ROS1 = ROS Proto-Oncogene 1, Receptor Tyrosine Kinase; RET = Ret Proto-Oncogene; PDGFRB = Platelet Derived Growth Factor Receptor Beta.
[a] See reference [35].

karyotype) and positive PLAG1 immunostaining, 4 with concordant negative results (lipoma-like subtypes), and 2 (a myxoid and classic subtype) with *HMGA2* rearrangements showing weak, focal PLAG1 staining that was interpreted as negative. The remaining 12 (48%) cases had molecular-immunohistochemical discrepancies, which were more evident in the lipoma-like lipoblastoma subtype. Of note, when *PLAG1* break-apart positive signal threshold was reduced from ≥9.93% to ≥6% of cells, the number of discrepancies decreased by 2 cases (Cases 13 and 16), rising the immunohistochemical to overall molecular concordance rate from 52% (13/25) to 60% (15/25).

4. Discussion

Our series consists of 28 lipoblastomas (17 of them confirmed by molecular techniques) with morphologic and immunohistochemical analysis. While other equally large studies had a major emphasis on morphology and immunophenotype [4,20], we sought to compare their immunohistochemical and molecular features, which has only been described in a smaller series of cases [6]. Similar to others, most of our cases (25/28, 89%) were identified within the first decade of life. In contrast to the largest series by Coffin et al (n = 59) reporting a spectrum of clinical associations in up to 17% of lipoblastomas [4], we did not identify any syndromic associations in our cohort.

The histologic diagnosis of lipoblastoma is relatively straightforward in tumors of infancy and early childhood with classic morphology; however, it may be challenging in limited biopsy specimens and unconventional presentations, likely requiring further ancillary confirmation. In early childhood, small biopsies mainly sampling mature lipomatous areas can elicit a wide spectrum of differential diagnoses, including lipofibromatosis, fibrous hamartoma of infancy, or even post-traumatic fat necrosis (ie post-traumatic pseudolipoma) (Table 2). Microscopically, lipofibromatosis may have a spindle cell component in fascicles, lacks lipoblasts, and shows a more infiltrative growth pattern with entrapment of surrounding tissues [1]. In cases of post-traumatic fat necrosis, clinical history is helpful in combination with the presence of chronic inflammatory changes, fat necrosis, and resolving hematoma formation [21]. Fibrous hamartoma of infancy can be more difficult to distinguish from lipoblastoma in biopsies lacking the characteristic primitive mesenchymal component and organoid appearance; however, their benign clinical course makes this distinction less crucial [1].

Although lipoblastomas can be distinguished from liposarcomas primarily based on age, unusual tumors in older children/young adults presenting with extensive myxoid or lipoma-like morphology and rare lipoblasts may prompt consideration of other differentials such as myxoid liposarcoma [1,5,9,13] and atypical lipomatous tumor/well-differentiated liposarcoma [10,22], which can be difficult to differentiate from lipoblastomas on histologic grounds when tissue material is limited, likely benefiting from further molecular confirmation. Additionally, insulin-induced lipoatrophy should be considered where clinical history of diabetes mellitus or starvation is present, as these cases can exhibit myxoid changes and pseudolipoblasts [23]. A list of pertinent differential diagnoses and key diagnostic findings is summarized in Table 2.

At the opposite age spectrum, infantile neoplasms predominantly composed of primitive mesenchymal cells with extensive myxoid stroma and minimal lipoblastic component would warrant consideration of a PMMTI, which portends a more aggressive behavior [24]. Although PMMTIs typically show cytologic atypia, increased mitotic activity, and a predominant round cell component in contrast to lipoblastomas, they can significantly overlap with the so-called group of "undifferentiated" myxoid lipoblastomas, as was recently reported by Warren et al [12]. Notably, the target RNA sequencing panel used here has been validated to assess *BCOR* internal tandem duplication, the characteristic alteration in PMMTI [25]. Although no *BCOR* ITDs were identified in this cohort, it is helpful to be able to simultaneously evaluate *PLAG1*, *HMGA2,* and *BCOR* in a single assay. Here, we also identified a lipoblastoma that was essentially composed of primitive spindle cells, extensive myxoid stroma, and absent lipoblastic elements, requiring further diagnostic confirmation by *PLAG1* FISH. In addition, we demonstrated that a subset of lipoma-like lipoblastomas harbor structural *PLAG1* rearrangements despite negative *PLAG1* FISH and immunohistochemistry, including a previously diagnosed lipoma.

In the modern molecular era, challenging cases benefit from additional ancillary testing by demonstrating *PLAG1* or rarely, *HMGA2* rearrangements. Currently, only a handful of *PLAG1* fusion partners have been identified in lipoblastomas (*HAS2*, *COL3A1*, *RAD51B*, *COL1A2*, and *RAB2A)*, all leading to overexpression of the *PLAG1* gene [3,5]. Here, we found a similar frequency of *PLAG1* rearrangements in lipoblastomas (60%) compared with prior series [6,7], while identifying 3 additional novel fusion partners (*DDX6*, *KLF10*, and *KANSL1L)*. Evidence suggesting that alternative fusion genes could be present in lipoblastomas has been noted in one previously reported case harboring an *HMGA2* fusion [15]. We identified 2 additional lipoblastomas harboring novel *HMGA2*

rearrangements with concordant moderate to strong HMGA2 protein expression. Interestingly, *HMGA2* is an upstream regulatory activator of *PLAG1* [26], and as such, it can induce activation and overexpression of PLAG1 in the absence of chromosome 8 abnormalities involving the *PLAG1* locus [26]. *HMGA2* fusions and *PLAG1* fusions are both known to occur in other entities, including pleomorphic adenoma [27], further reinforcing their shared biology. Our 2 *HMGA2*-rearranged cases were ultimately negative for PLAG1 immunohistochemistry albeit minimal expression was observed (1+, weak staining).

Interphase FISH testing is noted to be a highly reliable technique for the detection of the *PLAG1* fusion [3,6]. While all lipoblastomas underwent *PLAG1* FISH in our study, we found a substantial rate of unsuccessful testing in 6 lipoblastomas (21%). The reason for this high number of DNA-based test failures remains elusive; however, it may be related to the older age of the specimen (most failures occurring in specimens older than 10 years from original diagnosis), lipid-related autofluorescence [6], and formalin fixation time, as this variable was not controlled in our study. In addition, we identified several cases in which the *PLAG1* rearrangement was reported as negative by FISH, despite RNA sequencing proving otherwise, particularly among the group of lipoma-like lipoblastomas. This could be related, at least partially, to the positive signal threshold set for *PLAG1* translocation frequency by FISH. There is little consensus for an optimal cut-off signal in this setting, as most values have been determined in salivary gland tumors [6]. Interestingly, by decreasing the positive signal threshold from $\geq$9.93% to $\geq$6%, at least 2 additional lipoblastomas may have been correctly identified by FISH in our series with positive PLAG1 staining leading to a modest increase in the immunohistochemical to overall molecular concordance rate. Whether a lower diagnostic threshold for *PLAG1* FISH is more suitable in lipomatous tumors requires validation in further studies. Another potential explanation for the discrepancies is that the *PLAG1* rearrangement may not result in cytogenetic separation of the target gene in certain cases, which is a known pitfall of rearrangement detection by FISH [28,29]. Nonetheless, these observations underscore the value of RNA sequencing as an alternative confirmatory method in cases with unconventional features, including older pediatric/young adult patients with lipoma-like lesions and infants with diffusely myxoid lesions.

The frequency of PLAG1 protein expression in our series (40%) is lower than reported by others [2,9,12−14]. In myxoid and classic lipoblastomas, PLAG1 immunohistochemistry seems to be a better marker for *PLAG1* rearrangement as compared with lipoma-like subtypes. In lipoma-like subtypes, targeted RNA sequencing appears to best detect *PLAG1* fusions, as compared with FISH and immunohistochemistry. Historically, it has been suggested that lipoblastomas can evolve or "mature" to a conventional lipoma [6,8,15]. In our study, 6 lipoma-like lipoblastomas were negative for PLAG1 immunohistochemistry and *PLAG1* FISH despite harboring a *PLAG1* rearrangement demonstrated either by RNA sequencing or karyotype. Whether lipoma-like lipoblastomas represent a later stage of disease development into a "lipoma" rather than a distinct histologic variant requires further molecular characterization and comparison against a matched-group of morphologically designated pediatric lipomas.

Interestingly, we identified preferential nuclear expression of PLAG1 in mesenchymal cells within the myxoid stroma and fibrous septa, while showing less nuclear expression in mature adipocytes. These findings are similar to those reported in pleomorphic adenomas with differential staining in nuclei of myoepithelial and cartilaginous cells, whereas the lipomatous components lacked staining [30]. As it was proposed by Kubota et al, the consistent nuclear PLAG1 immunoreactivity of stromal and septal mesenchymal cells in lipoblastomas suggests their neoplastic nature and appears to correlate with simultaneous immunoreactivity to desmin [13], although this notion was not directly supported in our series. Remarkably, this preferential staining pattern in mesenchymal and fibroblast-like areas (some of which also demonstrated CD34 immunoreactivity) of lipoblastomas deserves further investigation. It is interesting to consider if the CD34+ fibroblastic "stem" cell may be the putative cell of origin for these tumors. Intriguingly, lipomatous tumors with a characteristic "fibroblastic" morphology have been recently reported as a novel morphologic variant of lipoblastoma occurring in adult patients [31], suggesting that their morphologic spectrum is broader than originally suspected as seen in one of our cases presenting as a recurrence (Case 2). It is still unclear if lipoblastomas share a common histogenesis with myofibroblastic tumors containing an adipose component (ie fibrous hamartoma, lipofibromatosis) as it was hypothesized in the past [6]. However, *EGFR* alterations in fibrous hamartomas of infancy [32] and kinase-related rearrangements in lipofibromatosis [33] might affect the primitive mesenchymal cells via activation of *PI3K−AKT−mTOR* paralleling the activating effects of *PLAG1* rearrangements on *MAPK* and *PI3K-AKT* signaling pathways by directly increasing expression of IGF2 [34](Fig. 5).

The main limitation of our study relies on its retrospective nature precluding consistent molecular confirmatory studies in all our cases and conduction of a more detailed sensitivity and specificity analysis among different diagnostic techniques. However, this series supports the notion that PLAG1 immunohistochemistry can be used in combination with other molecular ancillary studies for diagnostic confirmation of lipoblastomas with unconventional features and unusual presentations. While PLAG1 immunohistochemistry and *PLAG1* FISH appear to be more reliable in myxoid and classic lipoblastoma subtypes, RNA sequencing appears to have a better overall utility for lipoma-like subtypes and in those cases when first-line

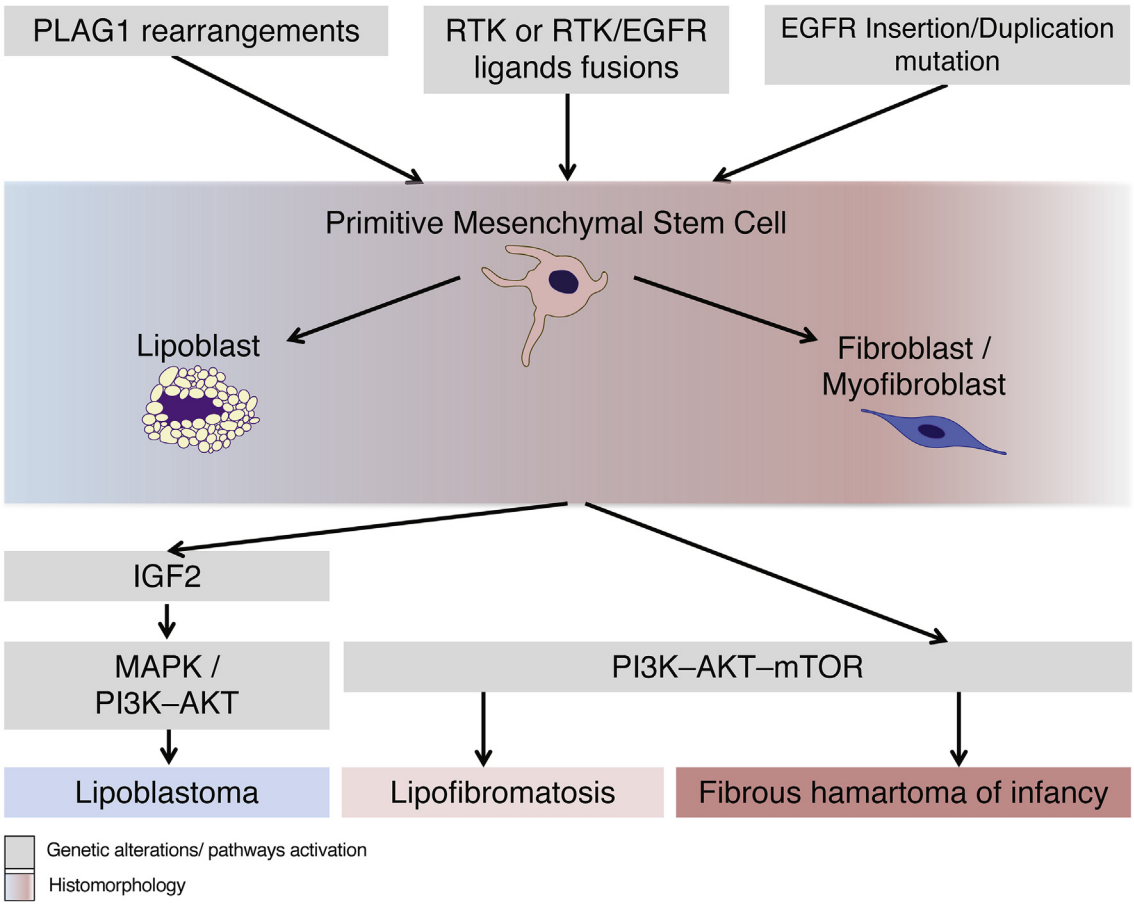

Fig. 5 Schematic of proposed common primitive CD34+ mesenchymal cell undergoing *PLAG1* rearrangements or other genetic alterations as a hypothesis for primitive cell potential to differentiate into adipose or fibroblastic cells resulting in a broad spectrum of morphologies ranging from myxoid or fibrous to frankly lipoma-like tumors.

testing (ie PLAG1 immunostain or FISH) is negative or borderline positive. RNA sequencing also identified cases with novel *HMGA2* fusions, which were negative for PLAG1 immunohistochemistry and *PLAG1* rearrangements by FISH. Opportune identification of associated genetic alterations and molecular classification of these pediatric lesions is important for appropriate follow-up and potential recurrences at an older age, which are particularly frequent in lipoblastomas [4]. Finally, the preferential PLAG1 protein expression in mesenchymal cells within myxoid and fibrous stroma, together with the differential expression of desmin and CD34 in mesenchymal cells deserves further investigation as these observations may suggest a CD34-positive primitive mesenchymal cell as the putative cell of origin in lipoblastomas. Our study shows that any pediatric lipomatous or myxoid-rich neoplasm harboring *PLAG1* rearrangements or alternative chromosomal alterations related to this gene locus, regardless of age, should be considered as part of the same spectrum of lipoblastomas.

Appendix ASupplementary data

Supplementary data to this article can be found online at https://doi.org/10.1016/j.humpath.2020.07.016.

Acknowledgments

The authors would like to thank Dr. Marian Harris and the Laboratory for Molecular Pediatric Pathology (LaMPP) at Boston Children's Hospital for their collaboration with targeted RNA sequencing on the Solid and Brain Tumor Fusion Panel, as well as UPMC Pathology FISH Laboratories, UPMC Children's Hospital of Pittsburgh Pathology Laboratory staff, and Mr. Christopher Woods, professional illustrator and application specialist at Cincinnati Children's Hospital Medical Center who provided technical support and expertise in the preparation of figures.

The authors thank Ms. Shannon Valenti, Regulatory Compliance Facilitator at the University of Pittsburgh

Clinical and Translational Science Institute (CTSI) for her assistance in the background preparation of this study.

Oscar Lopez-Nunez contributed to data curation, morphologic and immunohistochemical interpretation, writing (original draft preparation, revision/edition); Rita Alaggio contributed to conceptualization and study design, morphologic and immunohistochemical interpretation, critical manuscript revision/edition; Sarangarajan Ranganathan contributed to morphologic and immunohistochemical interpretation, critical manuscript revision/edition; Lori Schmitt contributed to methodology; Ivy John contributed to critical manuscript revision/edition; manuscript revision. Alanna J. Church contributed to methodology, molecular interpretation, critical manuscript revision/edition; Jennifer Picarsic contributed to conceptualization and study design, morphologic and immunohistochemical interpretation, critical manuscript revision/edition.

References

[1] Coffin CM, Alaggio R. Adipose and myxoid tumors of childhood and adolescence. Pediatr Dev Pathol 2012;15:239–54. https://doi.org/10.2350/10-05-0836-PB.1.

[2] Shinkai T, Masumoto K, Ono K, Yano E, Kobayashi C, Fukushima T, et al. A case of unusual histology of infantile lipoblastoma confirmed by PLAG1 rearrangement. Surg Case Rep 2015;1:42. https://doi.org/10.1186/s40792-015-0042-4.

[3] Hibbard MK, Kozakewich HP, Dal Cin P, Sciot R, Tan X, Xiao S, et al. PLAG1 fusion oncogenes in lipoblastoma. Cancer Res 2000;60:4869–72.

[4] Coffin CM, Lowichik A, Putnam A. Lipoblastoma (LPB): a clinicopathologic and immunohistochemical analysis of 59 cases. Am J Surg Pathol 2009;33:1705–12. https://doi.org/10.1097/PAS.0b013e3181b76462.

[5] Yoshida H, Miyachi M, Ouchi K, Kuwahara Y, Tsuchiya K, Iehara T, et al. Identification of COL3A1 and RAB2A as novel translocation partner genes of PLAG1 in lipoblastoma. Genes Chromosomes Cancer 2014;53:606–11. https://doi.org/10.1002/gcc.22170.

[6] Gisselsson D, Hibbard MK, Dal Cin P, Sciot R, Hsi BL, Kozakewich HP, et al. PLAG1 alterations in lipoblastoma: involvement in varied mesenchymal cell types and evidence for alternative oncogenic mechanisms. Am J Pathol 2001;159:955–62. https://doi.org/10.1016/S0002-9440(10)61771-3.

[7] Brandal P, Bjerkehagen B, Heim S. Rearrangement of chromosomal region 8q11-13 in lipomatous tumours: correlation with lipoblastoma morphology. J Pathol 2006;208:388–94. https://doi.org/10.1002/path.1879.

[8] Choi J, Bouron Dal Soglio D, Fortier A, Fetni R, Mathonnet G, et al. Diagnostic utility of molecular and cytogenetic analysis in lipoblastoma: a study of two cases and review of the literature. Histopathology 2014;64:731–40. https://doi.org/10.1111/his.12317.

[9] Matsuyama A, Hisaoka M, Hashimoto H. PLAG1 expression in mesenchymal tumors: an immunohistochemical study with special emphasis on the pathogenetical distinction between soft tissue myoepithelioma and pleomorphic adenoma of the salivary gland. Pathol Int 2012;62:1–7. https://doi.org/10.1111/j.1440-1827.2011.02740.x.

[10] Alaggio R, Coffin CM, Weiss SW, Bridge JA, Issakov J, Oliveira AM, et al. Liposarcomas in young patients: a study of 82 cases occurring in patients younger than 22 years of age. Am J Surg Pathol 2009;33:645–58. https://doi.org/10.1097/PAS.0b013e3181963c9c.

[11] Rotellini M, Palomba A, Baroni G, Franchi A. Diagnostic utility of PLAG1 immunohistochemical determination in salivary gland tumors. Appl Immunohistochem Mol Morphol 2014;22:390–4. https://doi.org/10.1097/PAI.0b013e3182936ea7.

[12] Warren M, Turpin BK, Mark M, Smolarek TA, Li X. Undifferentiated myxoid lipoblastoma with PLAG1-HAS2 fusion in an infant; morphologically mimicking primitive myxoid mesenchymal tumor of infancy (PMMTI)–diagnostic importance of cytogenetic and molecular testing and literature review. Cancer Genet 2016;209:21–9. https://doi.org/10.1016/j.cancergen.2015.11.004.

[13] Kubota F, Matsuyama A, Shibuya R, Nakamoto M, Hisaoka M. Desmin-positivity in spindle cells: under-recognized immunophenotype of lipoblastoma. Pathol Int 2013;63:353–7. https://doi.org/10.1111/pin.12077.

[14] Debelenko L, Henry C, Shivakumar B, Ar P-A, Kozakewich H. PLAG1 (pleomorphic adenoma gene 1) immunohistochemical expression in pediatric soft tissue and bone tumors and its role in diagnosis of lipoblastoma [Abstract]. Pediatr Dev Pathol 2009;12:321.

[15] Pedeutour F, Deville A, Steyaert H, Ranchere-Vince D, Ambrosetti D, Sirvent N. Rearrangement of HMGA2 in a case of infantile lipoblastoma without Plag1 alteration. Pediatr Blood Canc 2012;58:798–800. https://doi.org/10.1002/pbc.23335.

[16] Zheng Z, Liebers M, Zhelyazkova B, Cao Y, Panditi D, Lynch KD, et al. Anchored multiplex PCR for targeted next-generation sequencing. Nat Med 2014;20:1479–84. https://doi.org/10.1038/nm.3729.

[17] Roy S, Coldren C, Karunamurthy A, Kip NS, Klee EW, Lincoln SE, et al. Standards and guidelines for validating next-generation sequencing bioinformatics pipelines: a joint recommendation of the association for molecular Pathology and the college of American pathologists. J Mol Diagn 2018;20:4–27. https://doi.org/10.1016/j.jmoldx.2017.11.003.

[18] Jennings LJ, Arcila ME, Corless C, Kamel-Reid S, Lubin IM, Pfeifer J, et al. Guidelines for validation of next-generation sequencing-based oncology panels: a joint consensus recommendation of the association for molecular Pathology and college of American pathologists. J Mol Diagn 2017;19:341–65. https://doi.org/10.1016/j.jmoldx.2017.01.011.

[19] Paulson VA, Stojanov IA, Wasman JK, Restrepo T, Cano S, Plunkitt J, et al. Recurrent and novel USP6 fusions in cranial fasciitis identified by targeted RNA sequencing. Mod Pathol 2020;33:775–80. https://doi.org/10.1038/s41379-019-0422-6.

[20] Mentzel T, Calonje E, Fletcher CD. Lipoblastoma and lipoblastomatosis: a clinicopathological study of 14 cases. Histopathology 1993;23:527–33. https://doi.org/10.1111/j.1365-2559.1993.tb01238.x.

[21] Aust MC, Spies M, Kall S, Gohritz A, Boorboor P, Kolokythas P, et al. Lipomas after blunt soft tissue trauma: are they real? Analysis of 31 cases. Br J Dermatol 2007;157:92–9. https://doi.org/10.1111/j.1365-2133.2007.07970.x.

[22] Kuhnen C, Mentzel T, Fisseler-Eckhoff A, Debiec-Rychter M, Sciot R. Atypical lipomatous tumor in a 14-year-old patient: distinction from lipoblastoma using FISH analysis. Virchows Arch 2002;441:299–302. https://doi.org/10.1007/s00428-002-0690-1.

[23] Jermendy G, Nádas J, Sápi Z. "Lipoblastoma-like" lipoatrophy induced by human insulin: morphological evidence for local dedifferentiation of adipocytes? Diabetologia 2000;43:955–6. https://doi.org/10.1007/s001250051476.

[24] Alaggio R, Ninfo V, Rosolen A, Coffin CM. Primitive myxoid mesenchymal tumor of infancy: a clinicopathologic report of 6 cases. Am J Surg Pathol 2006;30:388–94. https://doi.org/10.1097/01.pas.0000190784.18198.d8.

[25] Santiago T, Clay MR, Allen SJ, Orr BA. Recurrent BCOR internal tandem duplication and BCOR or BCL6 expression distinguish

primitive myxoid mesenchymal tumor of infancy from congenital infantile fibrosarcoma. Mod Pathol 2017;30:884−91. https://doi.org/10.1038/modpathol.2017.12.

[26] Klemke M, Muller MH, Wosniok W, Markowski DN, Nimzyk R, Helmke BM, et al. Correlated expression of HMGA2 and PLAG1 in thyroid tumors, uterine leiomyomas and experimental models. PloS One 2014;9. https://doi.org/10.1371/journal.pone.0088126. e88126.

[27] Katabi N, Ghossein R, Ho A, Dogan S, Zhang L, Sung YS, et al. Consistent PLAG1 and HMGA2 abnormalities distinguish carcinoma ex-pleomorphic adenoma from its de novo counterparts. Hum Pathol 2015;46:26−33. https://doi.org/10.1016/j.humpath.2014.08.017.

[28] Chen S, Deniz K, Sung YS, Zhang L, Dry S, Antonescu CR. Ewing sarcoma with ERG gene rearrangements: a molecular study focusing on the prevalence of FUS-ERG and common pitfalls in detecting EWSR1-ERG fusions by FISH. Genes Chromosomes Cancer 2016; 55:340−9. https://doi.org/10.1002/gcc.22336.

[29] Argani P, Zhang L, Reuter VE, Tickoo SK, Antonescu CR. RBM10-TFE3 renal cell carcinoma: a potential diagnostic pitfall due to cryptic intrachromosomal Xp11.2 inversion resulting in false-negative TFE3 FISH. Am J Surg Pathol 2017;41:655−62. https://doi.org/10.1097/pas.0000000000000835.

[30] Matsuyama A, Hisaoka M, Nagao Y, Hashimoto H. Aberrant PLAG1 expression in pleomorphic adenomas of the salivary gland: a molecular genetic and immunohistochemical study. Virchows Arch 2011;458:583−92. https://doi.org/10.1007/s00428-011-1063-4.

[31] Fritchie K, Wang L, Horvai A, Torres-Mora J, Malik F, Folpe A, et al. Lipoblastomas presenting in older children and adults: analysis of 28 cases with identification of a new fibroblastic variant [Abstract]. In: United States & Canadian academy of Pathology 109th annual meeting; 2020. Los Angeles, California, USA.

[32] Park JY, Cohen C, Lopez D, Ramos E, Wagenfuehr J, Rakheja D. EGFR exon 20 insertion/duplication mutations characterize fibrous hamartoma of infancy. Am J Surg Pathol 2016;40:1713−8. https://doi.org/10.1097/pas.0000000000000729.

[33] Al-Ibraheemi A, Folpe AL, Perez-Atayde AR, Perry K, Hofvander J, Arbajian E, et al. Aberrant receptor tyrosine kinase signaling in lipofibromatosis: a clinicopathological and molecular genetic study of 20 cases. Mod Pathol 2019;32:423−34. https://doi.org/10.1038/s41379-018-0150-3.

[34] Andersson MK, Aman P, Stenman G. IGF2/IGF1R signaling as a therapeutic target in MYB-positive adenoid cystic carcinomas and other fusion gene-driven tumors. Cells 2019;8. https://doi.org/10.3390/cells8080913.

[35] WHO Classification of Tumors Editorial Board. Soft tissue and bone tumors, WHO classification of tumours series. 5th ed. Lyon, France: International Agency for Research on Cancer; 2020.